

Proton-Beam Writing of Poly-Methylmethacrylate Buried Channel Waveguides

T. C. Sum, *Member, IEEE*, A. A. Bettiol, Catalin Florea, *Member, IEEE*, and F. Watt

Abstract—In this paper, the authors report on the fabrication and characterization of poly-methylmethacrylate (PMMA) buried channel waveguides. The waveguides were fabricated using an emerging lithographic technique known as proton-beam writing. Depending on the proton fluence used, two different waveguide-formation mechanisms are possible. Single-mode waveguides with the light confinement occurring at the end of range were fabricated using fluences $< 75 \text{ nC/mm}^2$. The refractive-index profiles of these single-mode waveguides were recovered using the propagation mode near-field method. For fluences $> 100 \text{ nC/mm}^2$, multimode waveguides may also be fabricated with the light confinement occurring beneath the end of range. The compaction of the PMMA surface after proton irradiation was investigated using an atomic force microscope. The propagation losses of these PMMA waveguides were also determined.

Index Terms—Compaction, direct write, near-field mode profiles, PMMA buried channel waveguides, propagation mode near-field method, proton-beam writing, refractive-index profiles.

I. INTRODUCTION

ION implantation [1] is a well-established technique commonly used to modify the optical properties of a material. Compared to other waveguide-fabrication techniques, ion implantation offers the advantage of a precise depth control, at which the guides are formed. This can be done by controlling the energy of the ions. Ion implantation has been used to fabricate a wide range of optical waveguides [2]–[5]. Many of these materials used are crystals, doped glasses, etc., which are not as cost effective as polymers. Polymer optical waveguides offers an attractive low-cost solution for many telecommunication applications. In addition, their ease of processing and compatibility with other optical components allow them to be integrated into the same substrate [6].

The fabrication of optical waveguides in poly-methylmethacrylate (PMMA) using high-energy ion implantation has been previously reported [7], [8]. Ruck *et al.* [7] fabricated buried channel waveguides in PMMA using two methods: by irradiating the PMMA through a Si mask and by direct masking of the PMMA substrate using a Ni shim.

Manuscript received October 13, 2005; revised May 14, 2006. This work was supported by the Defence Innovative Research Programme (DIRP) Grant under the Defence Science and Technology Agency (DSTA), Singapore.

T. C. Sum is with the Division of Physics and Applied Physics, School of Physical and Mathematical Sciences, Nanyang Technological University, Singapore 637616 (e-mail: tzechien@ntu.edu.sg).

A. A. Bettiol and F. Watt are with the Department of Physics, Centre for Ion Beam Applications, National University of Singapore, Singapore 117542 (e-mail: phybaa@nus.edu.sg; phywattf@nus.edu.sg).

C. Florea is with the Sacks Freeman Associates (SFA), Inc., Crofton, MD 21114 USA (e-mail: cflorea@sfa.com).

Digital Object Identifier 10.1109/JLT.2006.881474

Hong *et al.* [8] used the ion implantation to fabricate planar waveguides in PMMA. These ion implantations were performed using a mask or by blanket irradiations of the substrate using an ion implanter. Channel waveguides require both lateral and transversal confinement. The former criterion can be fulfilled with the use of a mask or by means of direct write. The direct-write method is a more attractive option as it negates the need for an additional mask fabrication process, which may be tedious and expensive.

Proton-beam writing is an emerging lithographic technique, which uses a focused submicrometer beam of high-energy protons to direct write on suitable materials such as photoresists (e.g., SU-8, PMMA, etc) and inorganic materials (e.g., phosphate glass, Si, etc.). The technique is capable of fabricating SU-8 microstructures with smooth sidewalls [9]. This technique has applications in optical waveguide fabrication [10]–[12] as well as fabricating high-aspect ratio 100-nm metallic stamps [13] for nanoimprint lithography. Direct write using a focused megaelectronvolt proton beam to fabricate linear waveguides in fused silica has been previously reported [14], [15]. In contrast, proton-beam writing [16] is a dedicated lithographic technique with its own scanning software supporting a variety of design file formats (such as Autocad *.dxf). It is capable of fabricating waveguides of any arbitrary pattern and design.

The fabrication of y-branching waveguides in PMMA using the proton-beam writing was previously demonstrated [10]. However, only basic optical waveguide characterization results were reported, and no attempt was made to explain the mechanisms of the waveguide fabrication using the proton-beam writing. In this paper, we report on the fabrication and characterization of proton-beam-written buried channel PMMA waveguides. From the results on the surface compaction, the near-field mode profiles, and the recovered refractive-index profiles (using the propagation mode near-field method [17]–[19]), we seek to have a better understanding of the waveguide-formation mechanism of proton-beam-written PMMA buried channel waveguides.

II. EXPERIMENTAL

A. Waveguide Fabrication

Proton-beam writing is carried out using proton beams from the High Voltage Engineering Europa 3.5-MeV Singletron accelerator at the Center for Ion Beam Applications (CIBA) [20], Department of Physics, National University of Singapore. PMMA sheets from Röhm (Plexiglas GS233) of thickness $\sim 3 \text{ mm}$ were used in the fabrication of buried channel

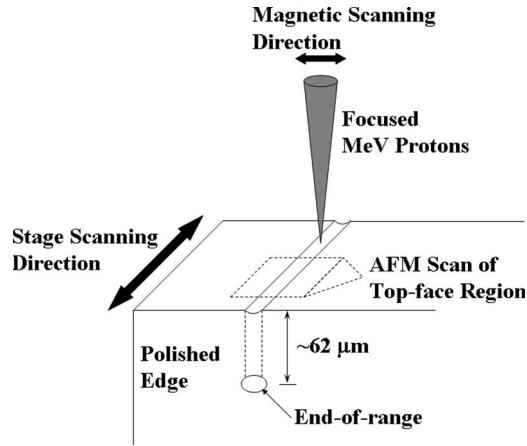


Fig. 1. Schematic of the proton-beam-writing process for the fabrication of PMMA buried channel waveguides.

waveguides. The fabrication was carried out using 2.0-MeV protons, which has a range of approximately $60 \mu\text{m}$ in PMMA. Linear buried channel waveguides of length $\sim 10 \text{ mm}$ were fabricated with fluences ranging from $30\text{--}125 \text{ nC/mm}^2$ (i.e., $1.9\text{--}7.8 \times 10^{13} \text{ particles/cm}^2$). The dose normalization procedure for proton-beam writing is based on the detection of backscattered protons. A description of the procedure can be found elsewhere [21].

A combination of stage scanning and magnetic scanning was used to direct write these waveguides. The proton beam was magnetically scanned over a distance of $5 \mu\text{m}$, while the stage was simultaneously traversed at a speed of $\sim 10 \mu\text{m/s}$, perpendicular to the magnetic scan direction. As the fabrication was carried out using focused megaelectronvolt protons, the high dose rate (i.e., the amount of protons delivered to the sample per unit area per unit time) might result in catastrophic damage to the PMMA (e.g., blistering and charring of the material). A beam current maintained at approximately 2 pA was used in the fabrication. Multiple irradiation loops were performed until the desired fluence is attained. Fig. 1 shows a schematic of the proton-beam-writing technique for the fabrication of linear PMMA buried channel waveguides. Unlike the proton-beam writing of SU-8 waveguides [11], there is no chemical development step for these PMMA waveguides.

B. Waveguide Characterization

After the proton-beam-writing process, the compaction of the irradiated pathways on the PMMA sample top face was assessed using a tapping mode atomic force microscope (AFM)—Digital Instruments Dimension 3000 SPM. The AFM scans were performed with the slow scan axis of the AFM probe aligned parallel to the irradiated pathways. The region of interest is illustrated schematically in Fig. 1. The end faces of the sample were edge polished using “chemo-mechanical” polishing (with diamond slurries and colloidal silica suspension) until the end faces of the waveguides were exposed with a roughness of less than 60 nm . The waveguides were end fire coupled by means of free-space coupling (using microscope objectives) as well as fiber coupling. The near-field mode profiles of the PMMA waveguides were imaged using a $50\times$ long

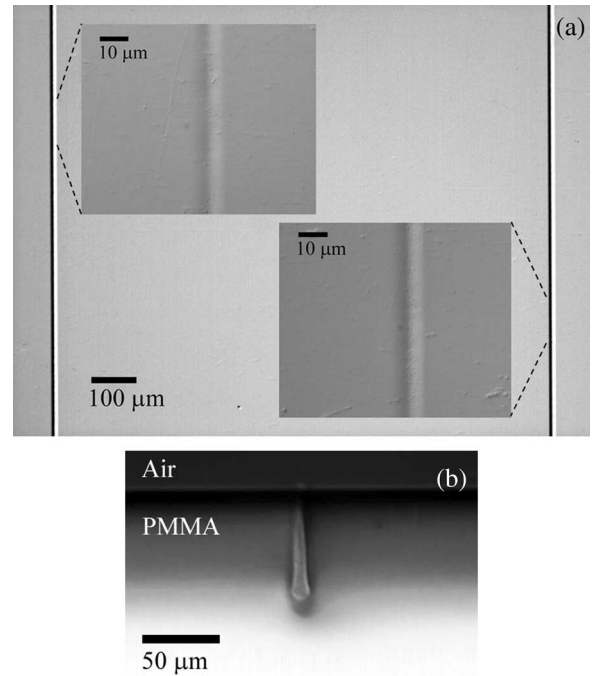


Fig. 2. (a) DIC image of the fabricated waveguides (top view). (b) Cross-sectional view of the polished waveguide endface. The waveguide was fabricated using a fluence of $\sim 100 \text{ nC/mm}^2$.

working distance microscope objective (N.A. = 0.42, resolving power $\sim 0.7 \mu\text{m}$) mounted on an InfiniTube in-line assembly and connected to a 12-bit charge-coupled-device (CCD) camera—Q-Imaging RETIGA EXi Digital CCD Camera. The refractive-index profiles of the single-mode PMMA buried channel waveguides were also recovered using the propagation mode near-field method (also known as the scalar wave inversion technique). The propagation losses of the PMMA waveguides were determined by measuring the intensity of the scattered light along the whole length of the waveguide using the same CCD camera.

III. RESULTS

Fig. 2(a) shows a differential-interference-contrast (DIC) micrograph of a pair of PMMA waveguides. A cross-sectional view of the end face of one of the waveguides is given in Fig. 2(b).

A. Measurement of Surface Compaction Using an AFM

An illustration of the surface compaction of the PMMA top face along the irradiated pathways is given in Fig. 3(a). The AFM images were flattened using a low-order polynomial fit. Such manipulation of raw AFM data is usually performed to remove the image artifacts (i.e., vertical offsets between scan lines), which may be caused by vertical (Z) scanner drift, image bow, or any nonlinear behavior in the piezo scanning mechanism. The average surface compaction of the waveguides as a function of proton fluence is given in Fig. 3(b). Each data point was averaged over five independent measurements over

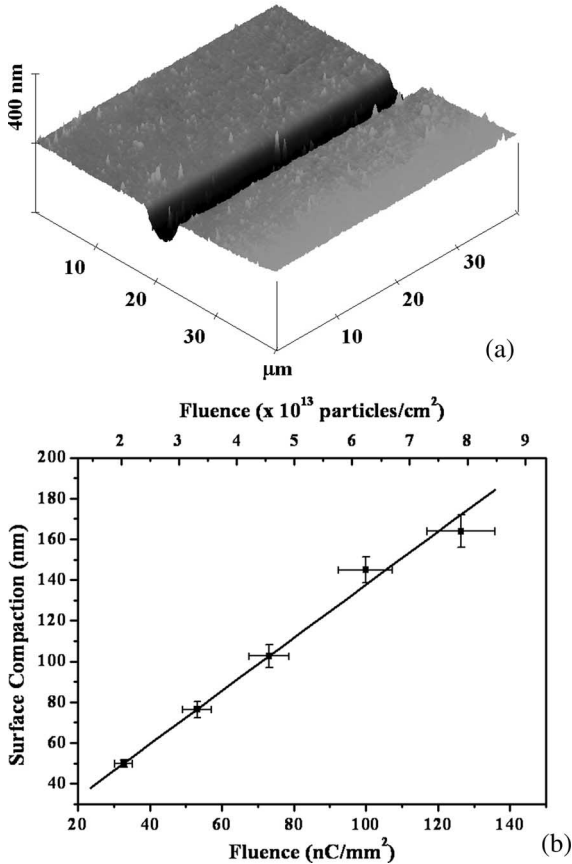


Fig. 3. (a) AFM image of the top face of one of the waveguides fabricated using a fluence of ~ 50 nC/mm². (b) Plot of the surface compaction as a function of the incident proton fluence.

arbitrary regions along the irradiated pathways. The data were subsequently fitted by a linear least square fit.

B. Near-Field Mode Profiles

Fig. 4(a)–(e) shows the near-field images of the mode profiles of the PMMA waveguides at 632.8 nm. The fabricated PMMA waveguides were found to be single mode and located at a depth of approximately 60 μm beneath the surface, in agreement with structural reaction injection molding stopping and range of ions in matter (SRIM) [22] simulations. A schematic is given in Fig. 4(f). Only the waveguides fabricated using the fluences of 32.8, 53.2, and 73.1 nC/mm² appear single moded and exhibit good mode confinement. The presence of a regular structure in the near-field mode profiles between the end of range and the surface of the substrate is believed to be a consequence of the interference due to a scattered light being reflected from the surface of the substrate. The modes of those guides fabricated using fluences > 100 nC/mm² appear “distorted” and irregularly shaped, exhibiting poor light confinement at the end of range. On the other hand, it was found that for these waveguides, the light confinement was achieved in the region beneath the end of range (by moving the coupling fiber down), as shown in Fig. 5(b) and (d). However, these mode profiles appear to be multimode. A schematic of the approximate location is given in Fig. 5(e). This effect is not observed for guides fabricated with the lower fluences.

C. Refractive-Index-Profile Reconstruction

The refractive-index profiles of the single-mode PMMA waveguides (i.e., waveguides fabricated with fluences < 75 nC/mm²) were recovered using the propagation-mode near-field method [17]–[19]

$$\Delta n(x, y) = -\frac{\nabla^2 \sqrt{I(x, y)}}{2n_s k_0^2 \sqrt{I(x, y)}}. \quad (1)$$

The second-order derivatives found in (1) require good mode-profile data with low noise. Averaging of the mode profiles and maximizing the signal to noise ratio (SNR) by exposing the CCD array for as long as possible without saturating the CCD pixels were some of the precautions taken. In addition, the average image of the mode profile was filtered using a Butterworth low-pass filter with a transfer function of $H(w) = \sqrt{1/(1+w^4)}$. A Matlab (The MathWorks Inc.) program was written to perform the necessary low-pass filtering and the subsequent recovery of the refractive-index profile $\Delta n(x, y) = n(x, y) - N_{\text{eff}}$. The propagation-mode near-field technique was first tested on a commercial fiber, and the recovered refractive-index profile was found to be in good agreement with the manufacturer’s specifications.

The bulk refractive index n_s of pristine PMMA was measured using a prism coupler and was found to be 1.490 at 632.8 nm. The normalized intensity profile of a PMMA waveguide fabricated with a fluence of ~ 33 nC/mm² is shown in Fig. 6(a), and the recovered index change (Δn) is given in Fig. 6(b). The e^{-2} intensity diameter of ~ 5.7 μm and a peak refractive-index change $\Delta n \sim 3.1 \times 10^{-3}$ were measured for a PMMA waveguide fabricated using a fluence of ~ 33 nC/mm². The two-dimensional (2-D) lateral and depth plots of the normalized intensity and the recovered profile mentioned above are given in Fig. 7(a) and (b). The Δn as a function of fluence was plotted in Fig. 8. The peak refractive-index change of the PMMA waveguides fabricated using fluences of 32.8–73.1 nC/mm² ranges from 3.1 – 4.8×10^{-3} .

D. Propagation-Loss Measurement

The propagation losses were measured for the three waveguides exhibiting good mode confinement (i.e., guides fabricated with fluences < 100 nC/mm²). A typical propagation-loss dependence as a function of length at 632.8 nm for PMMA waveguide fabricated using ~ 50 nC/mm² is given in Fig. 9. By averaging over ten independent measurements, the propagation loss as a function of the proton fluence was found to be 1.4 ± 0.2 dB/cm.

IV. DISCUSSIONS

Upon irradiation by 2.0-MeV protons, using fluences ranging from approximately 30–125 nC/mm² (i.e., 1.9 – 7.8×10^{13} particles/cm²), PMMA undergoes chain scission [23]. This results in the modification of the physical [23] and optical properties [7], [24] of PMMA. The analysis of the outgassing reaction products from PMMA during ion-beam

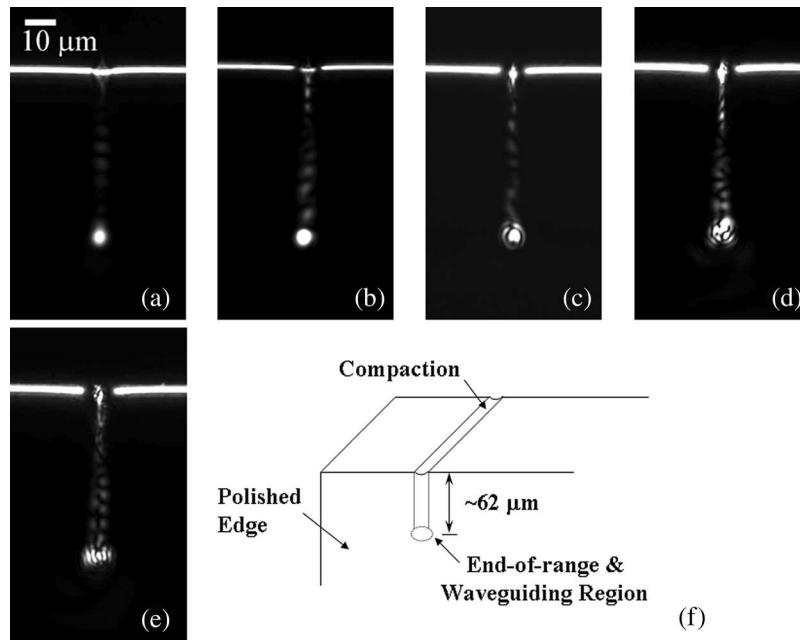


Fig. 4. Near-field mode profiles of the PMMA waveguides fabricated with different fluences at 632.8 nm. (a) 32.8 nC/mm². (b) 53.2 nC/mm². (c) 73.1 nC/mm². (d) 99.9 nC/mm². (e) 126.4 nC/mm². (f) Schematic illustrating the approximate location of the waveguiding region.

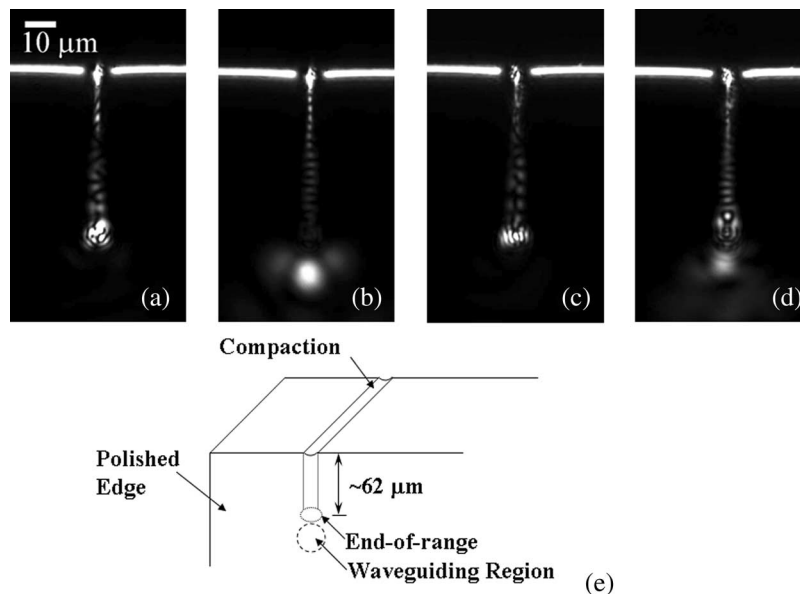


Fig. 5. Comparison of the near-field mode profiles of the PMMA waveguides at (a) and (c) end-of-range region and (b) and (d) region beneath it. The guides were fabricated with fluences (a) 99.9 nC/mm² and (c) 126.4 nC/mm². (e) Schematic illustrating the approximate location of the waveguiding region.

irradiation was previously reported by Ruck *et al.* [7]. The compaction of PMMA after ion irradiation is attributed to the following processes [25]: The stripping of the backbone of the monomer is induced by the energy transfer of the ions, which is indicated by the outgassing of the side groups as well as the formation of the O–H groups. Scission of the backbone also occurs, and this leads to the formation of CH₃ groups and C=C double bonds. From the AFM data shown in Fig. 3(b), the surface compaction of PMMA increases as the proton fluence increases, which is consistent with the above reported processes. The refractive index of isotropic polymers is related

to the physical and chemical properties by the Wei adaptation of the Lorentz–Lorenz relation [8]

$$\frac{\Delta n}{n} = \frac{(n^2 - 1)(n^2 + 2)}{6n^2} \left[-\frac{\Delta V}{V} + \frac{\Delta \alpha}{\alpha} + F \right] \quad (2)$$

where Δn refers to the change in refractive index, ΔV refers to the change in volume, α is the atomic bond polarisability, and F is the structure factors. The compaction of the irradiated PMMA (i.e., $-\Delta V$) causes the local densification of the

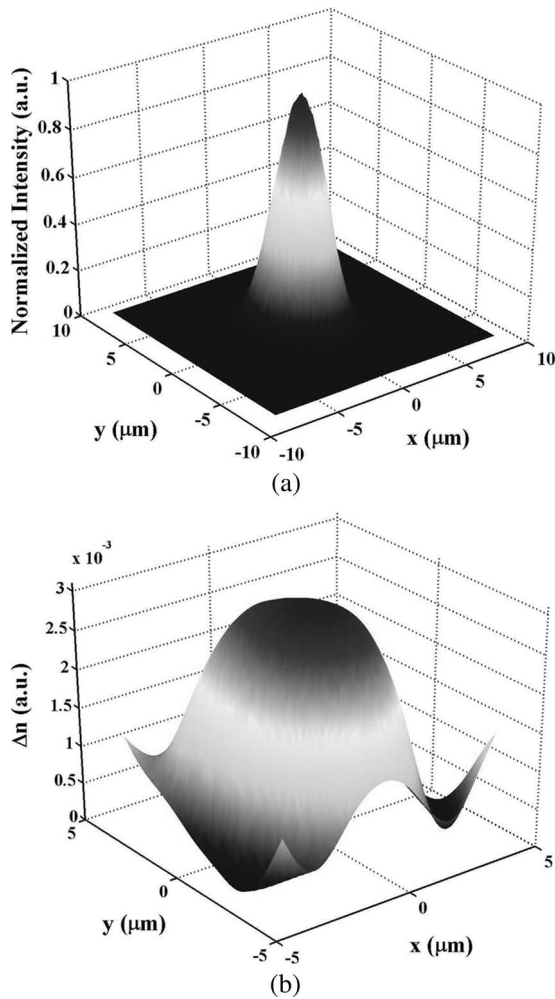


Fig. 6. (a) Normalized single-mode near-field profile (at 632.8 nm) of a proton-beam-written PMMA waveguide fabricated using a fluence of $\sim 33 \text{ nC/mm}^2$. (b) The recovered Δn of the same waveguide.

PMMA [24], [25], thus increasing the refractive-index change (i.e., $+\Delta n$).

From SRIM simulations, a beam of 2.0-MeV protons has a range of $\sim 60 \mu\text{m}$ in PMMA. The energy deposition due to the passage of ions through a polymer is mainly due to electronic stopping. Near the end-of-range region where the ion has sufficiently slowed down, there is a maximum deposition of energy, thus causing the largest modification to the PMMA. Waveguides fabricated using the fluences $< 75 \text{ nC/mm}^2$ exhibit good mode confinement at the end of range. From the recovered refractive-index profiles, a positive refractive-index change (i.e., $+\Delta n$) was determined and was found to range between $3.1 - 4.8 \times 10^{-3}$ for waveguides fabricated using fluences ranging from $32.8 - 73.1 \text{ nC/mm}^2$. The results for Δn are in agreement with those reported by Hong *et al.* [8] who fabricated planar PMMA waveguides using 1-MeV protons (with a fluence of $5 \times 10^{13} \text{ ions/cm}^2$) and measured their refractive indexes using the refracted near-field technique. A schematic illustrating the approximate location of the waveguiding region is given in Fig. 4(f).

For waveguides fabricated with fluences $> 100 \text{ nC/mm}^2$, poor light confinement at the end of range is observed. It is

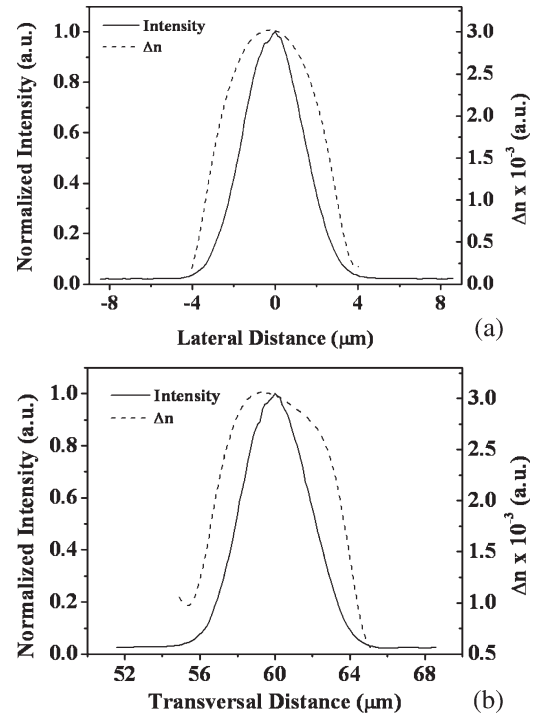


Fig. 7. (a) 2-D lateral plot of the normalized intensity (solid) and the recovered profile (dashed). (b) 2-D transversal (depth) plot of the normalized intensity (solid) and the recovered profile (dashed).

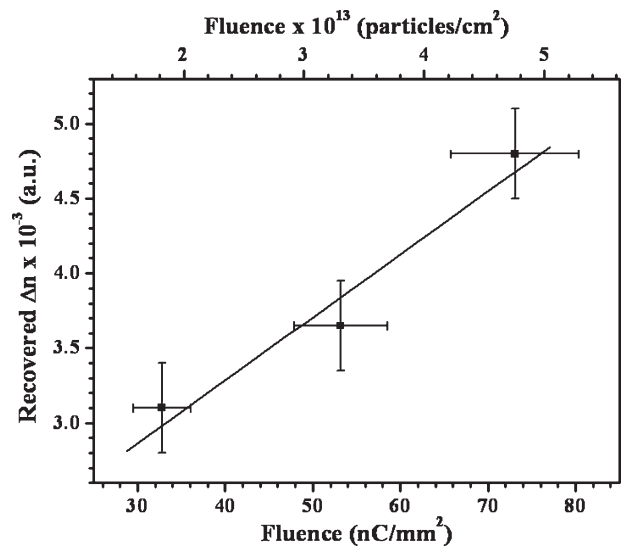


Fig. 8. Change in refractive index (Δn) as a function of fluence.

plausible that beyond this fluence, the high dose rate of the focused beam has caused “severe outgassing” of light organic fragments from the modified region. Microcavities of the trapped gases might also have been formed at the end of range, thus deteriorating the light confinement at the end of range. Alternatively, as the refractive index between the end of range and the surface of the substrate is increased by increasing fluence, the refractive-index difference between the end of range and the ion pathway would decrease. The end of range and the pathway could form a waveguide. This is consistent with the observation of standing waves between the end of range and the surface, as shown in Figs. 4 and 5. The waveguide formed at the end of

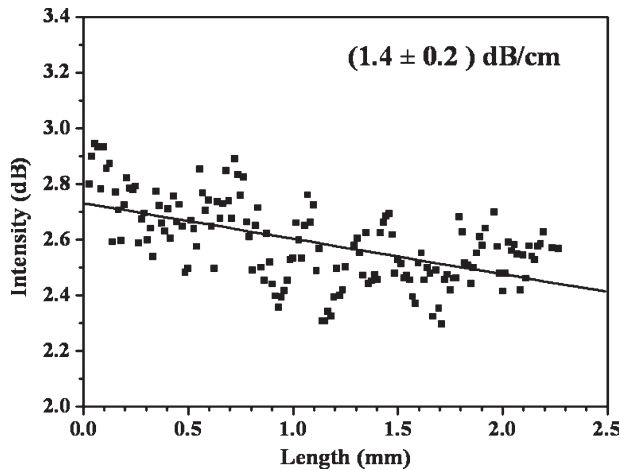


Fig. 9. Loss dependence of a PMMA waveguide fabricated using a fluence of ~ 50 nC/mm² at 632.8 nm.

range and the pathway has a larger vertical dimension; thus, it is possible that it is capable of supporting higher order modes. The irregularly shaped modes shown in Fig. 4(d)–(e) were obtained with the coupling fiber aligned at the end of range, and the manner at which the light was launched in this multimode waveguide may have brought about the excitation of higher order modes. Further investigation is required to understand the causes for the poor light confinement.

At these higher fluences, it is highly possible that a buildup of stress (from the modified or irradiated regions above the end of range) causes the compaction of the unmodified PMMA in the regions beneath the end of range. This interpretation is consistent with the observation of multimode waveguides shown in Fig. 5(b) and (d) at the region beneath the end of range (4–5 μ m below). Fig. 5(a) and (b) shows a comparison between the modes obtained for a guide fabricated using a fluence of ~ 100 nC/mm², with the coupling fiber at the end of range [Fig. 5(a)] and in the region beneath the end of range [Fig. 5(b)]. Similarly, the modes for a guide fabricated with a fluence of ~ 126 nC/mm² are compared in Fig. 5(c) and (d). Unless a careful comparison of the modes is performed, this effect can be easily overlooked due to the close proximity of the two waveguiding regions. A schematic depicting the approximate location is given in Fig. 5(e). No attempt was made to recover the refractive index as the propagation-mode near-field method is only applicable to single-mode waveguides. Such a phenomenon was not observed for waveguides fabricated with lower fluences. This null observation may be attributed to the insufficient compaction of the unmodified PMMA in the regions beneath the end of range (for guides fabricated with lower fluences).

PMMA waveguides fabricated with fluences ≤ 50 nC/mm² (i.e., $\leq 3.1 \times 10^{13}$ particles/cm²) exhibit propagation losses of ~ 1.5 dB/cm at 632.8 nm. At higher fluences, the propagation loss increases, indicating that the waveguides have become more lossy. This is probably attributed to the increased amount of “damage” of the polymer at higher fluences, which is consistent with the earlier interpretation of the deteriorating light confinement. Hong *et al.* [8] previously reported propagation losses of ~ 1.2 dB/cm at 635 nm for planar PMMA waveguides

fabricated using 350 keV H⁺ implantation with fluences of $\sim 2 \times 10^{14}$ particles/cm². These results indicate that the propagation losses for PMMA waveguides are highly dependent on the implantation conditions (i.e., focused beam, dose rate, beam energy and implantation fluence, etc.). It is possible that PMMA waveguides with even lower propagation losses can be fabricated using proton-beam writing. A more comprehensive study is required to establish the optimum fabrication conditions for proton-beam writing of low-loss PMMA buried channel waveguides.

V. CONCLUSION

In summary, PMMA buried channel waveguides were fabricated using an emerging lithographic technique known as proton-beam writing. Depending on the fluence used in the fabrication, two different waveguide-formation mechanisms are possible. Single-mode waveguides were fabricated using fluences ranging from 30–75 nC/mm². Light confinement for these waveguides occurs at the end of range where the maximum energy from the proton beam is deposited. It is believed that the increase in refractive index was brought about by the compaction of the PMMA after irradiation, thus increasing the local density of the modified region, which in turn increases the refractive index. The refractive-index profiles of these single-mode waveguides were recovered using the propagation-mode near-field method. For waveguides fabricated using fluences > 100 nC/mm², multimode waveguides were fabricated with the light confinement occurring in the region beneath the end of range. It is believed that the stress buildup from the compaction of the modified regions (i.e., regions above the end of range) increases the density of the material beneath the end of range, thus increasing the refractive index. However, poor mode confinement in the end of range is observed for these waveguides. The surface compaction was also investigated using an AFM and was found to increase linearly with fluence. Propagation losses of ~ 1.5 dB/cm at 632.8 nm were also measured for the PMMA waveguides fabricated with fluences ≤ 50 nC/mm².

ACKNOWLEDGMENT

The authors would like to thank S. Venugopal Rao for the technical assistance rendered to parts of the optical characterization setup.

REFERENCES

- [1] P. D. Townsend, P. J. Chandler, and L. Zhang, *Optical Effects of Ion Implantation*. Cambridge, U.K.: Cambridge Univ. Press, 1994, ch. 6.
- [2] F. X. Wang, F. Chen, X. L. Wang, Q. M. Lu, K. M. Wang, D. Y. Shen, H. J. Ma, and R. Nie, “Fabrication of optical waveguides in KTiOAsO₄ by He or Si ion implantation,” *Nucl. Instrum. Methods Phys. Res. B, Beam Interact. Mater. At.*, vol. 215, no. 3/4, pp. 389–393, Feb. 2004.
- [3] G. Fu, K. M. Wang, F. Chen, X. L. Wang, S. L. Li, D. Y. Shen, H. J. Ma, and R. Nui, “Extraordinary refractive-index increase in MeV B³⁺ ion-implanted LiNbO₃ waveguide,” *Nucl. Instrum. Methods Phys. Res. B, Beam Interact. Mater. At.*, vol. 211, no. 3, pp. 346–350, Nov. 2003.
- [4] P. Moretti, M. F. Joubert, S. Tascu, B. Jacquier, M. Kaczkan, M. Malinowskii, and J. Samecki, “Luminescence of Nd³⁺ in proton or helium-implanted channel waveguides in Nd:YAG crystals,” *Opt. Mater.*, vol. 24, no. 1/2, pp. 315–319, Oct./Nov. 2003.

- [5] F. Chen, X. L. Wang, X. S. Li, L. L. Hu, Q. M. Lu, K. M. Wang, B. R. Shi, and D. Y. Shen, "Ion-implanted waveguides in Nd³⁺-doped silicate glass and Er³⁺/Yb³⁺ co-doped phosphate glass," *Appl. Surf. Sci.*, vol. 193, no. 1–4, pp. 92–101, Jun. 2002.
- [6] L. Eldada and L. W. Shacklette, "Advances in polymer integrated optics," *IEEE J. Sel. Topics Quantum Electron.*, vol. 6, no. 1, pp. 54–68, Jan./Feb. 2000.
- [7] D. M. Ruck, S. Brunner, K. Tinschert, and W. F. X. Frank, "Production of buried waveguides in PMMA by high energy ion implantation," *Nucl. Instrum. Methods Phys. Res. B, Beam Interact. Mater. At.*, vol. 106, no. 1–4, pp. 447–451, Dec. 1995.
- [8] W. Hong, H. J. Woo, H. W. Choi, Y. S. Kim, and G. D. Kim, "Optical property modification of PMMA by ion-beam implantation," *Appl. Surf. Sci.*, vol. 169–170, pp. 428–432, Jan. 2001.
- [9] T. C. Sum, A. A. Bettiol, H. L. Seng, J. A. van Kan, and F. Watt, "Direct measurement of proton-beam-written optical sidewall morphology using an atomic force microscope," *Appl. Phys. Lett.*, vol. 85, no. 8, pp. 1398–1400, Aug. 2004.
- [10] T. C. Sum, A. A. Bettiol, H. L. Seng, I. Rajta, J. A. van Kan, and F. Watt, "Proton beam writing of passive waveguides in PMMA," *Nucl. Instrum. Methods Phys. Res. B, Beam Interact. Mater. At.*, vol. 210, pp. 266–271, Sep. 2003.
- [11] T. C. Sum, A. A. Bettiol, J. A. van Kan, F. Watt, E. Y. B. Pun, and K. K. Tung, "Proton beam writing of low-loss polymer optical waveguides," *Appl. Phys. Lett.*, vol. 83, no. 9, pp. 1707–1709, Sep. 2003.
- [12] K. Liu, E. Y. B. Pun, T. C. Sum, A. A. Bettiol, J. A. van Kan, and F. Watt, "Erbium-doped waveguide amplifiers fabricated using focused proton beam writing," *Appl. Phys. Lett.*, vol. 84, no. 5, pp. 684–686, Feb. 2004.
- [13] K. Ansari, J. A. van Kan, A. A. Bettiol, and F. Watt, "Proton beam fabrication of nickel stamps for nanoimprint lithography," *Appl. Phys. Lett.*, vol. 85, no. 3, pp. 476–478, 2004.
- [14] A. Roberts and M. L. von Bibra, "Fabrication of buried channel waveguides in fused silica using focused MeV proton beam irradiation," *J. Lightw. Technol.*, vol. 14, no. 11, pp. 2554–2557, Nov. 1996.
- [15] M. L. von Bibra, A. Roberts, and S. D. Dods, "Ion beam energy attenuation for fabrication of buried, variable-depth, optical waveguides," *Nucl. Instrum. Methods Phys. Res. B, Beam Interact. Mater. At.*, vol. 168, no. 1, pp. 47–52, May 2000.
- [16] F. Watt, J. A. van Kan, and T. Osipowicz, "Three-dimensional microfabrication using maskless irradiation with MeV ion beams: Proton beam micromachining," *MRS Bull.*, vol. 25, no. 2, pp. 33–38, Feb. 2000.
- [17] K. Morishita, "Refractive-index-profile determination of single-mode optical fibers by a propagation-mode near-field scanning technique," *J. Lightw. Technol.*, vol. LT-1, no. 3, pp. 445–449, Sep. 1983.
- [18] —, "Index profiling of three-dimensional optical waveguides by the propagation-mode near-field method," *J. Lightw. Technol.*, vol. LT-4, no. 8, pp. 1120–1124, Aug. 1986.
- [19] M. L. von Bibra and A. Roberts, "Refractive index reconstruction of graded-index buried channel waveguides from their mode intensities," *J. Lightw. Technol.*, vol. 15, no. 9, pp. 1695–1699, Sep. 1997.
- [20] F. Watt, J. A. van Kan, I. Rajta, A. A. Bettiol, T. F. Choo, M. B. H. Breese, and T. Osipowicz, "The National University of Singapore high energy ion nano-probe facility: Performance tests," *Nucl. Instrum. Methods Phys. Res. B, Beam Interact. Mater. At.*, vol. 210, pp. 14–20, Sep. 2003.
- [21] A. A. Bettiol, J. A. van Kan, T. C. Sum, and F. Watt, "A LabVIEW—Based scanning and control system for proton beam micromachining," *Nucl. Instrum. Methods Phys. Res. B, Beam Interact. Mater. At.*, vol. 181, no. 1–4, pp. 49–53, Jul. 2001.
- [22] J. F. Ziegler, J. P. Biersack, and U. Littmark, *Stopping and Range of Ions in Solids*. New York: Pergamon, 1985.
- [23] H. W. Choi, H. J. Woo, W. Hong, J. K. Kim, S. K. Lee, and C. H. Eum, "Structural modification of poly(methyl methacrylate) by proton irradiation," *Appl. Surf. Sci.*, vol. 169–170, pp. 433–437, Jan. 2001.
- [24] D. M. Ruck, J. Schulz, and N. Deusch, "Ion irradiation induced chemical changes of polymers used for optical applications," *Nucl. Instrum. Methods Phys. Res. B, Beam Interact. Mater. At.*, vol. 131, no. 1–4, pp. 149–158, Aug. 1997.
- [25] D. M. Ruck, "Ion induced modification of polymers at energies between 100 keV and 1 GeV applied for optical waveguides and improved metal adhesion," *Nucl. Instrum. Methods Phys. Res. B, Beam Interact. Mater. At.*, vol. 166–167, pp. 602–609, May 2000.

T. C. Sum (S'01–M'05) was born in Singapore in 1976. He received the B.Sc. (1st Class Hon.), M.Sc., and Ph.D. degrees in physics from the National University of Singapore in 1999, 2001, and 2005, respectively.

In 2005, he joined the School of Physical and Mathematical Sciences, Nanyang Technological University, Singapore, where he is currently a Lecturer. He is currently interested in femtosecond studies of energy transfer process: ultrafast time-resolved phenomena of excitons in semiconducting nanoparticles and organic light-emitting molecules.

A. A. Bettiol was born in Melbourne, Australia, in 1970. He received the B.Sc. (Hon.) and Ph.D. degrees in physics from University of Melbourne in 1992 and 2000, respectively.

He then joined the Centre for Ion Beam Applications, Department of Physics, National University of Singapore, as a Research Fellow. He is currently applying the proton-beam-writing technique to applications in microphotonics. In particular, his research interests include the fabrication of photonic crystals, microlens arrays, waveguides, and gratings.

Catalin Florea (S'97–M'02) was born in Bucharest, Romania, in 1972. He received the B.S. degree in physics from Bucharest University, in 1995, and the M.S. degree in electrical engineering and computer science and the Ph.D. degree in applied physics from The University of Michigan, Ann Arbor, in 1999 and 2002, respectively.

In 2002, he briefly joined Northstar Photonics, Minneapolis, MN, where he worked on ion-exchanged waveguide glass lasers for telecom applications. From 2002 to 2005, he was with IMRA America, Inc., Ann Arbor, where he worked on femtosecond fiber laser engineering and development. Currently, he is employed with SFA, Inc., Crofton, MD, as a Research Physicist for The Naval Research Laboratory, Washington, DC. His research interests include waveguide devices in rare earth-doped glass and lithium niobate, applications of femtosecond lasers, and chalcogenide-based fiber amplifiers and lasers.

Dr. Florea is a member of the Optical Society of America (OSA).

F. Watt was born in the U.K. in 1946. He received the B.Sc. and Ph.D. degrees from University of Newcastle upon Tyne, Newcastle upon Tyne, U.K., in 1967 and 1972, respectively.

From 1972 to 1992, he was a member of the Nuclear and Particle Physics Department, University of Oxford, Oxford, U.K., where he initiated and headed the scanning proton microprobe unit. In 1992, he moved to the National University of Singapore, Singapore, where he is currently a Professor of physics and the Director of the Centre for ion-beam applications.